RSC Advances

PAPER

View Article Online
View Journal | View Issue

Cite this: *RSC Adv.*, 2020, **10**, 19759

Synthesis and properties of a temperature-sensitive hydrogel based on physical crosslinking *via* stereocomplexation of PLLA-PDLA

Xiaoyu Shi,[ab] Jie Wu,[ab] Zhidan Wang,[ab] Fei Song,[ab] Wenli Gao[ab] and Shouxin Liu *[ab]

Received 25th February 2020
Accepted 12th May 2020

DOI: 10.1039/d0ra01790f

rsc.li/rsc-advances

A synthetic route to amphiphilic conetwork (APCN) gels was developed and involved (1) a ring-opening polymerization (ROP) synthesis of the macromonomer HEMA-PLLA/PDLA, and (2) a radical polymerization of a stereocomplex of the synthesized macromonomers with P(MEO_2MA-*co*-OEGMA) to form the APCN gels. The structure of the gel was successfully verified using X-ray diffraction. Thermal analysis and differential scanning calorimetry data showed that the thermal behaviors of the gels were greatly improved compared with that of polylactic acid (PLA). The mechanical properties of the gels were measured by using a dynamic viscometer, and the results indicated a greater mechanical strength before swelling than afterwards, and an increasing strength of the gels with increasing amount of PLA stereocomplex. Gels placed in different aqueous phases at different temperatures showed different swelling ratio (SR) values. Specifically, the SR gradually decreased as the temperature was increased, indicating a temperature sensitivity of the gels. In addition, the gels placed in the aqueous and organic phases presented as hydrogels and hydrophobic gels, respectively, and their SR values were relatively low. These results indicated the amphiphilic nature of the gel, and indicated great application prospects for the gel in biomedicine.

1. Introduction

Polylactic acid (PLA) is an important degradable polymer material. Its synthetic raw materials are obtained from renewable resources. After being used, it can be degraded into H_2O and CO_2, and hence introduce no pollution to the environment.[1–3] At present, polylactic has been widely used in controlled drug release, non-removable surgical sutures and microcapsules for injections, landfills, as support materials, and as repair materials in tissue engineering.[4] PLA forms two enantiomers: poly (L-lactide) (PLLA) and poly (D-lactide) (PDLA), which can form a racemate by hydrogen bonding, *i.e.*, the so-called stereocomplex.[5–7] Compared with the individual enantiomers, PLA stereocomplexes exhibit better physical properties, such as higher melting points, higher mechanical strength levels, and improved thermal and hydrolytic stability levels.[8–12] These unique characteristics are beneficial to the applications of PLA in biomedicine. Most importantly, using the PLA stereocomplex as a cross-linker has several advantages over other cross-linking methods, such as reaction under mild conditions and avoiding the use of catalysts, auxiliary crosslinking agents, and other active molecules.[13]

Poly(*N*-isopropylacrylamide) (PNIPAM) has been by far the most-studied thermoresponsive polymer in materials science. Indeed, this synthetic polymer exhibits a low critical solution temperature (LCST) of about 32 °C in aqueous medium and is, therefore, very useful for preparing smart materials for biological applications. However, in recent years, polymer chemists reported very interesting alternatives to PNIPAM.[14,15] Temperature-sensitive, water soluble biocompatible copolymers of 2-(2-methoxyethoxy) ethyl methacrylate (MEO_2MA) and oligo(ethylene glycol) methacrylate (OEGMA) have been widely studied. LCST values of 26 °C and 90 °C have been measured for PMEO_2MA and POEGMA, respectively—with the copolymers exhibiting LCSTs between these temperatures, and which can be precisely adjusted by varying the ratio of the amount of one co-monomer to that of the other.[16–18] P(MEO_2MA-*co*-OEGMA) has been extensively studied in drug delivery systems due to its excellent temperature response, and excellent hydrophilicity, biocompatibility and non-toxicity.

Amphiphilic conetwork (APCN) gels as a rapidly emerging new material, consist not only of hydrophilic polymer components, but also hydrophobic polymer components, which are covalently bonded together in a cross-linked macromolecular assembly.[19–22] APCN gels are more mechanically stable than are their pure homopolymeric analogues. Importantly, APCN gels have some extraordinary properties, such as swelling

[a]*Key Laboratory of Applied Surface and Colloid Chemistry (Shaanxi Normal University), Ministry of Education, Xi'an, 710062, PR China. E-mail: liushx@snnu.edu.cn; Tel: +86-29-81530781*

[b]*School of Chemistry & Chemical Engineering, Shaanxi Normal University, Xi'an 710062, PR China*

independent of solvent polarity, formation of a nanophase structure, excellent mechanical strength, and good biocompatibility, which make them promising for applications in a wide variety of areas.[23–30]

In this study, we successfully synthesized biocompatible APCN gels, namely the poly[2-(2-methoxyethoxy)ethyl-methacrylate-*co*-oligo(ethylene glycol)methacrylate]-*l*-stereocomplex of poly(L-lactide) and poly(D-lactide) (P[MEO_2MA-*co*-OEGMA]-*l*-*S*-(PLLA-PDLA)). First, physical cross-linking was accomplished *via* stereocomplexation of the macromonomers HEMA-PLLA and HEMA-PDLA, and then the hydrophilic monomers MEO_2MA and OEGMA were added to form the APCN gels. Hydrogels formed by physical crosslinking display better mechanical strengths and higher melting points than do hydrogels formed by chemical crosslinking.[31–34] Importantly, these materials were found to be biocompatible and degradable, which can promote their application in the field of biomedicine.

2. Experimental

2.1. Materials

2-Hydroxyethyl methacrylate (HEMA, M_n = 130.14 g mol^{-1}), 2-(2-methoxyethoxy) ethyl methacrylate (MEO_2MA, 95%, M_n = 188 g mol^{-1}) and oligo (ethylene glycol) methacrylate (OEGMA, 98%, M_n = 475 g mol^{-1}) were purchased from TCL (Shanghai Development Co., Ltd., Shanghai, China) and purified by passing them through a column with neutral alumina oxide to remove inhibitor. 2,2-Azoisobutyronitrile (AIBN) was purified by recrystallizing it from methanol. L-Lactide and D-lactide (M_n = 144.13 g mol^{-1}) were purchased from TCL (Shanghai Development Co., Ltd., Shanghai, China) and were purified by recrystallizing them from ethyl acetate. Dichloromethane (DCM) was dried by performing distillation with calcium hydride before use. Tetrahydrofuran (THF) containing NaOH was dried by performing distillation with benzophenone before use. 1,8-Diazabicyclo[5.4.0]undec-7-ene (DBU) (98%, Aldrich) was used as received.

2.2. Preparation of the amphiphilic conetwork gels

2.2.1. Synthesis of the macromonomer HEMA-PLLA. Under an atmosphere of dry nitrogen, 2-hydroxyethyl methacrylate (101 μL, 1 mmol), L-lactide (1.5614 g, 13 mmol), and dry DCM (20 mL) were added to a dried 50 mL round-bottom flask. The mixture was stirred until all monomers dissolved, and then DBU (20 μL 0.13 mmol) was injected into the system. After stirring the resulting mixture at room temperature overnight, the reaction was quenched by adding benzoic acid. The reaction mixture was concentrated, and then precipitated in hexane two times. The resulting polymer was dried under vacuum at 35 °C. (A similar method was used to synthesize the macromonomer HEMA-PDLA.)

2.2.2. Synthesis of amphiphilic conetwork gels (P[MEO_2MA-*co*-OEGMA]-*l*-*S*-(PLLA-PDLA)). The physically cross-linked amphiphilic conetworks were prepared by carrying out free radical copolymerization of the active PLA stereocomplex with 2-hydroxyethyl methacrylate. In a typical such preparation procedure, first the copolymers of HEMA-PLLA (0.0250 g, 0.0235 mmol) and HEMA-PDLA (0.025 g, 0.00235 mmol) and then OEGMA (64 μL, 31 mmol) and MEO_2MA (890 μL, 170.84 mmol) were placed into a 10 mL round-bottom flask; secondly, the resulting mixture was subjected to the action of ultrasound to cause a complete mixing and dissolution of the components and hence ensure the complete formation of the stereocomplex; and, finally, AIBN (0.1 g) was added to the system, and polymerization was performed at 70 °C for 30 min.

2.3. Structural characterization

2.3.1. Nuclear magnetic resonance (^{1}H NMR) spectroscopy. ^{1}H nuclear magnetic resonance (^{1}H NMR) spectra were recorded on a Bruker Ultrashield 300 MHz spectrometer (300 MHz AVANCE, Bruker Corporation, Germany) at room temperature using $CDCl_3$ as the solvent. Chemical shifts (δ) were given relative to tetramethylsilane (TMS).

2.3.2. Fourier transform infrared (FT-IR) spectroscopy. The infrared spectrum of the HEMA-PLLA macromonomer was acquired using a Bruker FTIR apparatus (Tensor 27, Bruker Corporation, Karlsruhe, Germany). Before the measurement, the dried sample was mixed with KBr, ground into a powder, and tableted.

2.3.3. X-ray diffraction (XRD) patterns. An X-ray diffractometer (XRD, Bruker D8 Advance) operating at a voltage of 40 kV and current of 40 mA and with Cu Kα radiation (λ = 0.15418 nm) was used to determine the formation of the stereocomplex. The powdery macromonomer and the gel were fully dried, and evenly placed on the glass slide. The X-ray data were recorded using a scanning angle ranging from 10° to 50° and a measuring speed of 3° min^{-1}.

2.4. Property measurements

2.4.1. Mechanical properties of the gels. The four newly prepared gels with different PLA polymerization degrees were placed in deionized water for 4 days, and then disk-shaped gel samples were made using a punch and denoted as P1, P2, P3 and P4, respectively. The storage moduli of the gels were determined by carrying out compression experiments using a dynamic viscometer (Q800DMA of TA Company, USA). The creep test of P3 was performed under different stresses to determine the elasticity levels of the hydrogels.

2.4.2. Thermal properties of the gels. Thermogravimetric analysis is one of the methods available to determine the thermal properties of gels. The thermogravimetric data of the dried gels were collected using a Thermoanalyzer Systems apparatus (TA-Waters Q600, USA). The samples with masses of 5–10 mg were weighed separately, and then were heated from 25 °C to 600 °C with a scanning rate of 10 °C min^{-1}. Differential scanning calorimetry analysis (DSC Mettler-Toledo DSC1) is another method to determine the thermal properties of gels; here, the temperature and heat flow were calibrated with standard indium. The gels were sufficiently dried, and samples with masses of 3–5 mg were weighed separately. The samples were

then equilibrated at 25 °C, and then ramped up at 10 °C min^{-1} to 350 °C, and the total heat flow was recorded.

2.4.3. Swelling studies. The gels (dried using a freeze dryer) were placed in (1) deionized water at pH = 7, 25 °C; or (2) in an organic phase. They were taken out at regular intervals, the surface solvent was wiped with filter paper, and they were quickly weighed. The swelling ratio (SR) was calculated using the formula

$$SR = (W_t - W_d)/W_d,$$

where W_d is the weight of the original dry gel and W_t is the weight of the swollen gel at time t.

2.4.4. Temperature sensitivity, de-swelling and reversible swelling of the gels. Hydrogels that had reached a swelling equilibrium were placed in deionized water at either (1) pH = 7, 20–42 °C or (2) pH = 7, 42 °C. The mutation temperature and de-swelling kinetics of the gels were measured. After a fixed time interval, the surface moisture was wiped with a filter paper and the samples were weighed quickly. The de-swelling degree was calculated using the formula

$$SR = (W_t - W_d)/W_s,$$

where W_d is the weight of the original dry gel, W_t is the weight of the swollen gel at time t, and W_s is the weight of the gel after complete swelling.

In addition, the P3 hydrogel after having reached swelling equilibrium was placed in a water bath at pH = 7, 42 °C. After 30 minutes, it was taken out, and the surface moisture was wiped prior to weighing the sample. The sample was then put into a water bath at pH = 7, 22 °C again, and taken out after 30 minutes, had its surface moisture wiped off, and was then weighed. The above operation was repeated multiple times over the course of about 5 hours. The reversible swelling of the gel was calculated by using the above formula.

2.4.5. DSEM images of cross-sections of the gels. The gels of the different samples were placed into a pH 7, 25 °C water bath and left in there until their swellings reached full equilibrium. At those points, they were quickly frozen with liquid nitrogen to maintain the good gel shape, and then a freeze dryer (FD-27 Detianyou) was used to dry the gels. A desktop scanning electron microscope (TM3030 Hitachi) was used to obtain images of the cross-sections of the gels in high vacuum mode. (In order to improve the conductivity of the gels, the gels were sprayed with gold for 90 s.)

3. Results and discussion

3.1. Characterization of polymers and gels

3.1.1. Syntheses of the polymers and gels. In this study, macromolecular monomers and gels were synthesized by performing ring-opening polymerization (ROP) and free radical polymerization. First, L-lactide (or D-lactide) ring opening was reacted with 2-hydroxyethyl methacrylate by using the catalyst DBU to obtain the product HEMA-PLLA as shown in Scheme 1. The obtained macromonomers HEMA-PLLA and HEMA-PDLA

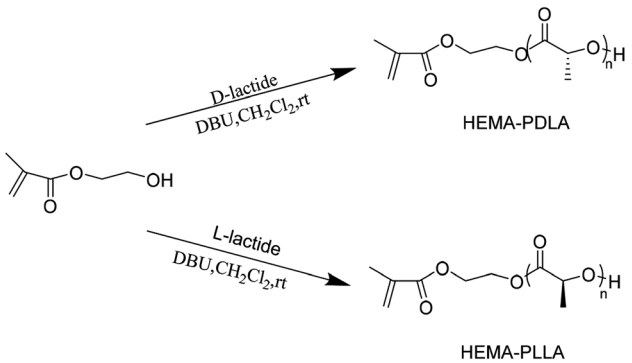

Scheme 1 Synthesis routes to macromonomers HEMA-PLLA/HEMA-PDLA.

were thoroughly stirred under the action of ultrasonication, and they were physically cross-linked *via* PLA stereocomplexes. After the addition of the hydrophilic substances MEO_2MA and OEGMA, the synthesis of the gel was carried out under the action of the initiator AIBN. The synthesis route is shown in Scheme 2. The composition of the gel was controlled by controlling the feed ratio of the PLLA/PDLA blend (see Table 1).

3.1.2. Structure of the macromonomer HEMA-PLLA. The acquired ^{1}H NMR spectrum of HEMA-PLLA is shown in Fig. 1(a). The methyl proton peaks at 1.35–1.54 ppm can be assigned to –(C=O)–CH–(CH_3). The methyl proton peak at 2.01 ppm can be assigned to CH_3–. The active hydrogen peak at 3.3–3.4 ppm can be assigned to –CH–(CH_3)–OH. The methylene proton peak at 4.3 ppm can be assigned to –O–CH_2–. The methine proton peak at 5.1 ppm can be assigned to –(C=O)–CH–(CH_3). The peaks at 5.5 ppm and 6.2 ppm are the absorption peaks of the –(CH_3)C=CH_2 methylene proton. The molecular weight of HEMA-PLLA (HEMA-PDLA) was calculated from the ^{1}H NMR spectra by using the formula[13]

$$M_{n\ NMR} = \frac{A_d}{A_{a+b}} \times 72 + 130$$

where A_{a+b} and A_d stand for the integral areas of peaks (a+b) and (d), respectively. The values of 72 and 130 are the molecular weights of the repeat units of PLLA and the macroinitiator HEMA, respectively.

As shown in Fig. 1(b), the infrared absorption spectrum of HEMA-PLLA showed various absorption peaks: at 1195 cm^{-1},

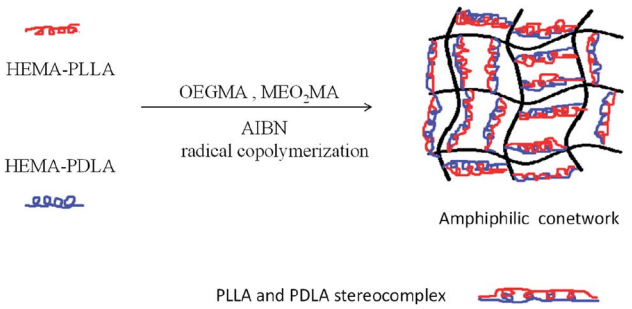

Scheme 2 Synthesis route to the amphiphilic conetwork gel.

Table 1 Synthesis data for the copolymers

Samples	HEMA/PLLA(PDLA) (n : n)	OEGMA/MEO_2MA (n : n)	HEMA-PLLA/HEMA-PDLA (W : W)	W^a : W^b (%)
P1	1 : 9	5 : 95	1 : 1	1 : 5
P2	1 : 13	5 : 95	1 : 1	1 : 5
P3	1 : 16	5 : 95	1 : 1	1 : 5
P4	1 : 20	5 : 95	1 : 1	1 : 5

[a] 1 : 1 mixtures of macromonomers HENA-PLLA and HEMA-PDLA. [b] 5 : 95 mixtures of OEGMA and MEO_2MA.

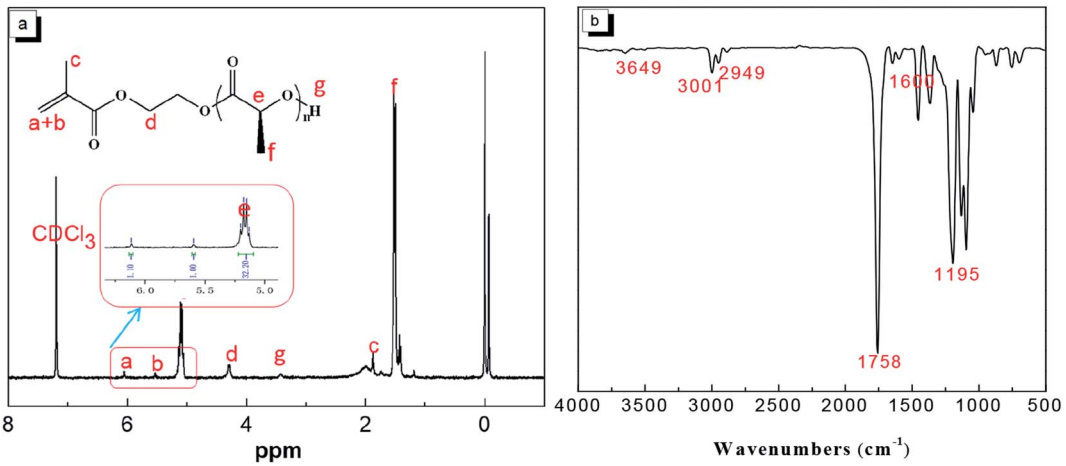

Fig. 1 (a) The acquired ^1H NMR and (b) IR spectra of HEMA-PLLA.

characteristic of –COC–; at 1600 cm^{-1}, characteristic of –C=C–; a characteristic peak of C=O at 1758 cm^{-1}; characteristic peaks of $-CH_2$, $-CH_3$ at 3001 cm^{-1} and 2949 cm^{-1}; and a characteristic peak of –OH at 3649 cm^{-1}. The nuclear magnetic resonance and infrared spectra of HEMA-PDLA were observed to be essentially identical to those of HEMA-PLLA.

3.1.3. Structures of the gels. X-ray diffraction (XRD) was used to verify the existence of PLA stereocomplexes in the polymer co-network.[35–39] Fig. 2 shows the acquired XRD patterns of the macromolecular monomer HEMA-PLLA, the polymer without complete stereocomplexing of PLA, and the stereocomplexed PLA gel. As shown in curve (a) of the figure, HEMA-PLLA yielded diffraction peaks at $2\theta = 15.8°$, 18.2°, and 19.8°, which corresponded to PLLA, and the peak shapes were sharp and narrow, indicating the high crystallinity of HEMA-PLLA. (PDLA showed similar results.) As shown in curve (b) of the figure, the polymer without complete stereocomplexing of PLA no longer showed the characteristic diffraction peak of the macromolecular monomer, and the diffraction peaks that were observed were significantly wider than those for the monomer. This result was attributed to the addition of the hydrophilic substance modifying the hydrophobic PLLA, and the polymer developing a relatively amorphous structure. As shown in curve (c) of the figure, diffraction peaks again appeared at $2\theta = 12°$ and 21° in the pattern produced by the stereocomplexed PLA gel, and the peak shapes were sharp and narrow, confirming the presence of PLA stereocomposite crystals.

3.2. Properties of the gels

3.2.1. Mechanical strength levels of the gels. The curves obtained using dynamic mechanical analysis (DMA) of the

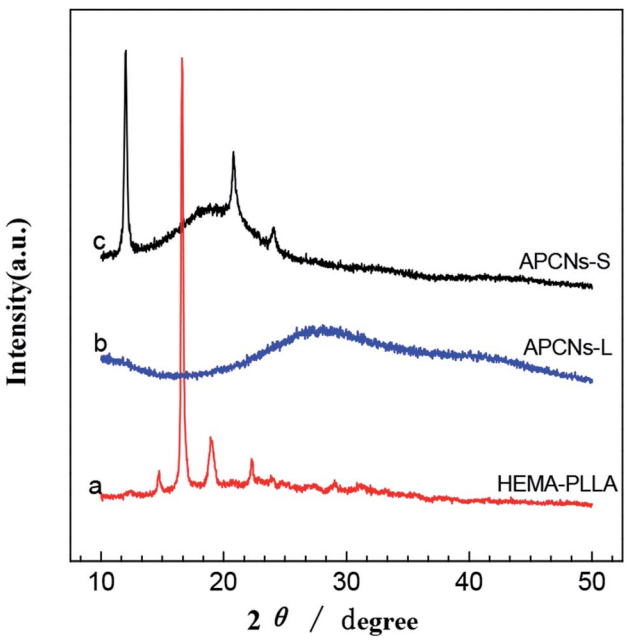

Fig. 2 . The acquired XRD patterns of the macromolecular monomer HEMA-PLLA (a), the polymer without complete stereocomplexing of PLA (b), and the stereocomplexed PLA gel (c).

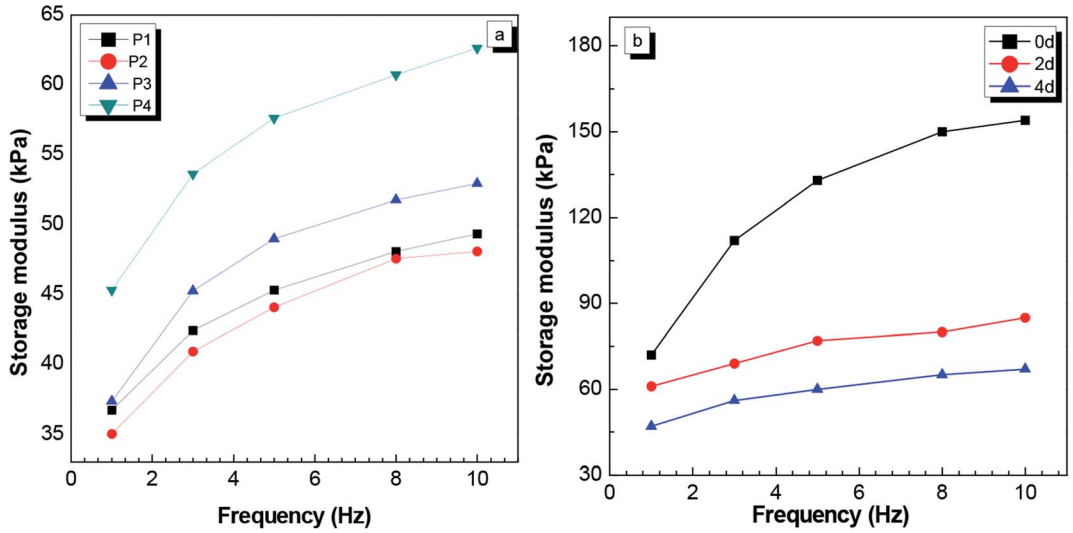

Fig. 3 (a) Dynamic mechanical analysis (DMA) curves of the P1, P2, P3, P4 gels after swelling for 4 days. (b) The P3 DMA curves after swelling for 0 d, 2 d and 4 d in distilled water.

different gels after 4 days of swelling are shown in Fig. 3(a). These curves reflected the mechanical properties of the gels. The four curves showed the same trend, with the storage modulus increasing with frequency. Also as clearly seen in the figure, the storage modulus values of the hydrogels increased with PLA polymerization degree. When the frequency was 10 Hz, the storage modulus values of the gels were 49.34 kPa, 48.07 kPa, 52.92 kPa and 62.63 kPa, respectively. This result was due to higher amounts of stereocomplexes of PLA being associated with more points of action for forming hydrogen bonds between PLLA and PDLA, and hence gels with smaller pores and less likely to collapse. DMA curves of the P3 gel swelling in deionized water at different times are shown in Fig. 3(b). For a frequency of 10 Hz, these curves indicated a storage modulus of 154 kPa for the dry gel, and modulus decreasing continuously from this level with increasing swelling time, specifically to 85 kPa at 2 days and 67 kPa at 4 days. This experiment provided strong evidence for the high mechanical strength of the gels and of the great impact of swelling time on their strength and elasticity levels. The longer the swelling time, the larger the pores of the gel, and the easier it apparently was to break the gel, resulting in the relatively poor gel strength and elasticity. (The experiment was repeated three times to ensure the accuracy of the data.)

At 25 °C, P3 was subjected to constant stresses of 6 kPa, 8 kPa and 10 kPa. Inspection of the corresponding creep curves (displayed in Fig. 4) showed the gel strain changing with time, reflecting the extensibility of the gels. When the applied stress was 10 kPa, the gels showed a great strain of 23%; and when the applied stresses were 8 kPa and 6 kPa, the strains were sequentially reduced to 19% and 16%, respectively. After the stress was removed, the deformation the gel was observed to diminish. Obviously, the greater the stress, the smaller was the recovered strain. The experimental results showed a certain level of elasticity displayed by the hydrogel, and as the stress was increased, the elasticity of the gel gradually decreased. (The experiment was repeated three times to ensure the accuracy of the data (Fig. 5).)

3.2.2. Thermal properties of the gel. The thermal stability of the gel was evaluated by performing thermogravimetric analysis. The thermal degradation temperature refers to the temperature of the first weight loss. Fig. 6 shows the thermogravimetric curves for different gels. These curves showed that all of the gels began to lose weight at 220–280 °C, indicative of their relatively high thermal stability levels. Clearly, as described above, the greater the applied stressed, the smaller was the strain recovered. And the thermogravimetric analysis showed

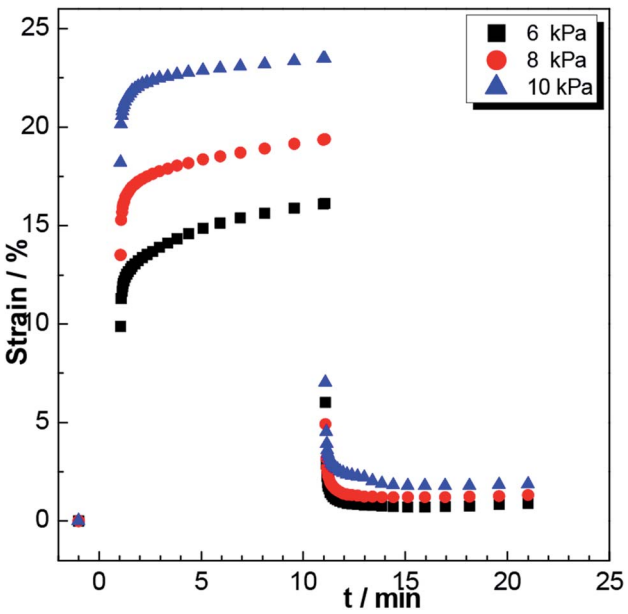

Fig. 4 Curves of strain *versus* time for P3 gels subjected to constant stresses of 6 kPa, 8 kPa and 10 kPa.

Fig. 5 Photographs of unstretched (top) and stretched (bottom) P3 gels. The photographs were taken with a digital camera.

higher phase change temperatures for gels with higher degrees of PLA polymerization, specifically 220 °C for P1 and 280 °C for P4. The higher observed decomposition temperatures of the gels with greater degrees of PLA polymerization were attributed to these gels having more hydrogen bonding interactions between PLLA and PDLA molecules.

Further evidence for the relatively high thermal stability levels of our gels was provided by the results of DSC analysis. As shown in Fig. 7, the DSC results of the gels indicated two typical physical transitions: a glass transition at a temperature (T_g) close to 180 °C and crystal melting at a temperature (T_m) roughly in the vicinity of 280 °C. The crystal melting peak was due to the successful stereocomplexation of PLLA and PDLA and the presence of SC crystallites. Moreover, with the increase of the degree of PLA polymerization, the T_m value gradually increased, completely consistent with the results of the thermogravimetric analysis. The glass transition temperature (T_g) did not much vary from 180 °C as the PLA polymerization degree was increased, indicating little effect of the stereocomplex on the movement of the segments in the blend.

3.2.3. Swelling studies. One of the most interesting properties of our amphiphilic conetworks was their abilities to swell in both polar and nonpolar solvents. Some dry gel samples were transferred into deionized water and others into THF, and allowed to swell until they reached equilibrium. The masses of the swollen gels were measured and used to calculate the SR values. The swelling kinetics curves of the P1, P2, P3 and P4 gels placed in deionized water with a pH of 7 at 25 °C are shown in Fig. 8(a). These curves showed similar trends for P1, P2, P3 and P4, with SR gradually increasing with time, but gradually decreasing with the increasing degree of PLA polymerization.

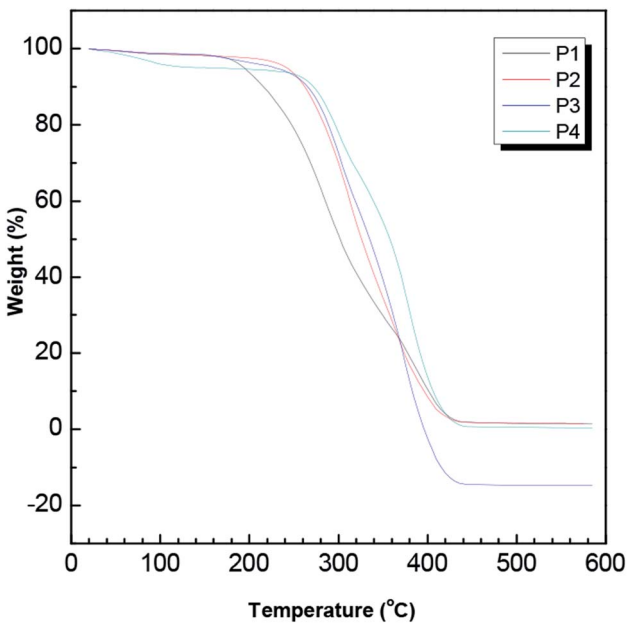

Fig. 6 The acquired thermogravimetric curves of various gels.

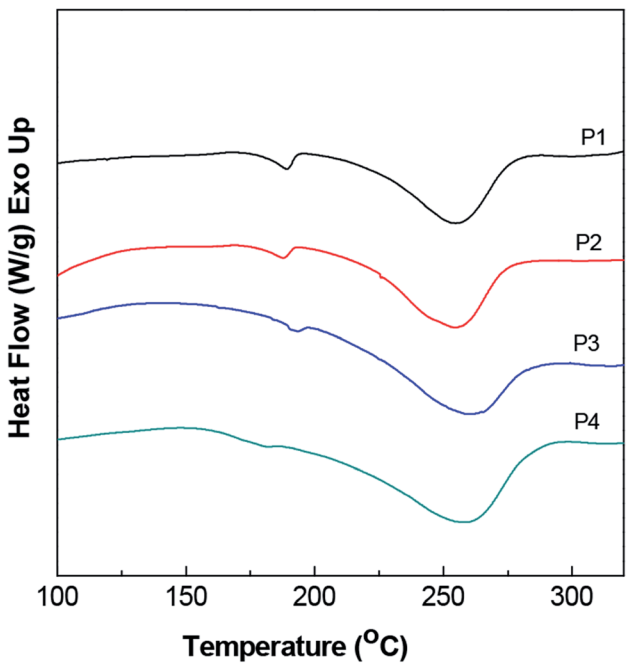

Fig. 7 The acquired DSC curves of the PLLA/PDLA blends with different contents.

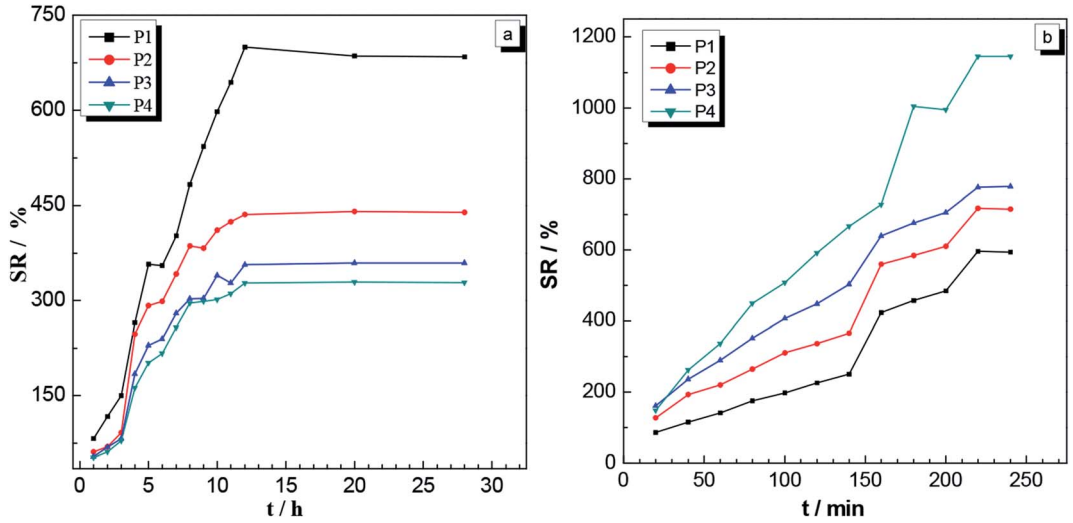

Fig. 8 Swelling ratios as a function of time for the P1, P2, P3 and P4 gels placed in (a) deionized water at 25 °C and pH 7, and (b) THF.

Table 2 Results of swelling of gels in different solvents

Swelling degree (%)				
Sample	H_2O	CH_3OH	THF	DCM
P1	692 ± 12	212 ± 28	593 ± 25	928 ± 22
P2	436 ± 15	253 ± 23	715 ± 36	1312 ± 24
P3	357 ± 8	283 ± 20	778 ± 21	1307 ± 18
P4	328 ± 10	318 ± 37	1144 ± 29	1533 ± 32

The swelling kinetics curves of the P1, P2, P3 and P4 gels in THF are shown in Fig. 8(b). These curves also showed overall trends, *i.e.*, increasing SR with time, similar to each other and to those of the gels in the aqueous phase—but interestingly, in THF, the gel SR gradually increased with the increasing degree of PLA polymerization. This result was attributed to the gels in the organic phase being related to the degree of PLA polymerization: the greater the amount of the hydrophobic substance, the more organic points of action, and the greater was the SR. We also examined gels in different solvents as shown in Table 2. The gels swelled in both polar and different nonpolar solvents. That is, these new materials were shown to display amphiphilic characters. Thus, depending on their outer environment, these conetworks could behave either as hydrogels (in the presence of water) or hydrophobic gels (in case of hydrophobic, nonpolar solvents). Besides, it can be clearly seen from the figure that whether the gels swelled in the aqueous phase or the organic phase, the SR values of the gels were relatively small. Placement of these gels in the body would thus not be expected to cause local edema, and the use of such gels has led to great progress in the field of drug delivery.[23] (The experiment was repeated three times to ensure the accuracy of the data.)

Fig. 9 shows pictures of the gel taken with a digital camera. Panel (A) shows a picture of the untreated gel; panel (B) shows a picture of the gel after it was completely swollen in a deionized water bath at pH 7, 25 °C; and panel (C) shows a picture of the gel after it was swollen in THF. Inspection of these photographs also showed that the gels swelled in both the aqueous phase and the organic phase, completely consistent with the results in Fig. 8(a) and (b), thus further illustrating the amphiphilic natures of the gels.

3.2.4. Temperature sensitivities of the gels. In order to determine the low solution critical temperature (LCST) values of

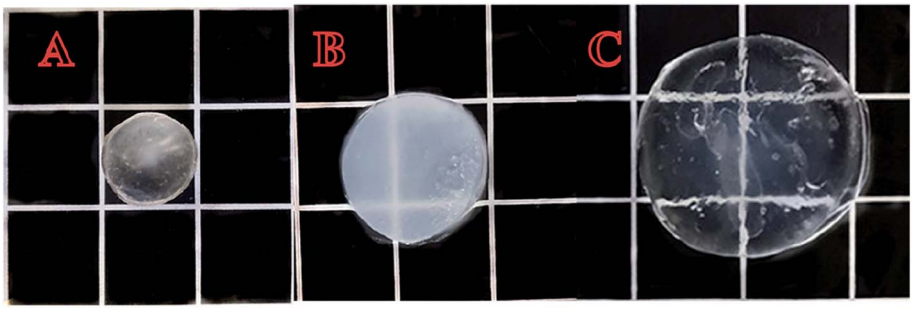

Fig. 9 Photographs taken with a digital camera of (A) an untreated gel, (B) gel completely swollen in a deionized water bath at pH 7, 25 °C and (C) gel swollen in THF.

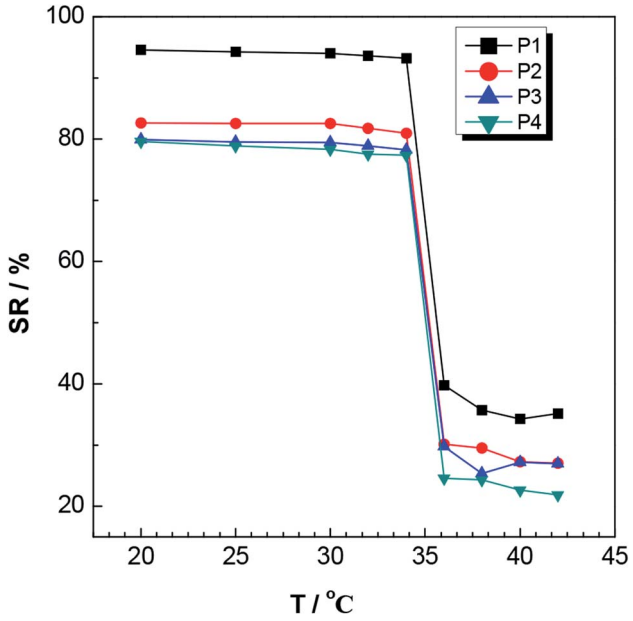

Fig. 10 Swelling ratios of the four gels at various temperatures.

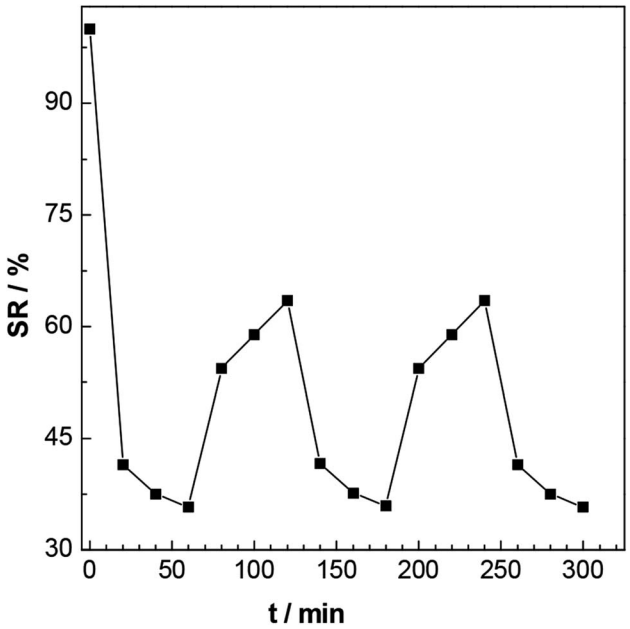

Fig. 12 The swelling and de-swelling of the P3 gel in deionized water at 25 °C and 42 °C (see text).

the gels, their SR values were determined at various temperatures from 20–42 °C, and at 30 minutes when they presumably reached swelling equilibrium. As shown in Fig. 10, the gels showed relatively constant and high degrees of swelling at temperatures lower than 35 °C. But when the temperature was increased from just below 35 °C to just above this temperature, the swelling degree markedly decreased, to as low as about 20%. As the temperature was further increased, the swelling degrees remained relatively constant at this low level. Therefore, the mutation point temperature of the gels was 35 °C. (The experiment was repeated three times to ensure the accuracy of the data.)

3.2.5. Swelling and de-swelling dynamics of the gels. Swelling kinetics curves of the P1, P2, P3, and P4 gels in deionized water at pH = 7, 25 °C are shown in Fig. 11(a). These curves were observed to be similar to each other, with the swelling degree increasing rapidly with time during the first 15 h and gradually so after 15 h. At swelling equilibrium, the swelling degrees of the P1, P2, P3 and P4 gels were 692%, 435.5%, 356.6% and 328.77%, respectively. Due to the formation of the gel mainly depending on hydrogen bonding between PLLA and PDLA, the lower the PLA polymerization degree of the gel, the fewer hydrogen bonding points present between PLLA and PDLA, and the larger were the pores of the gel network structure. Therefore, the degree of swelling of P1 was the greatest. At 25 °C, hydrogels that had reached swelling equilibrium were immersed in a pH 7 water bath at 40 °C (T > LCST)

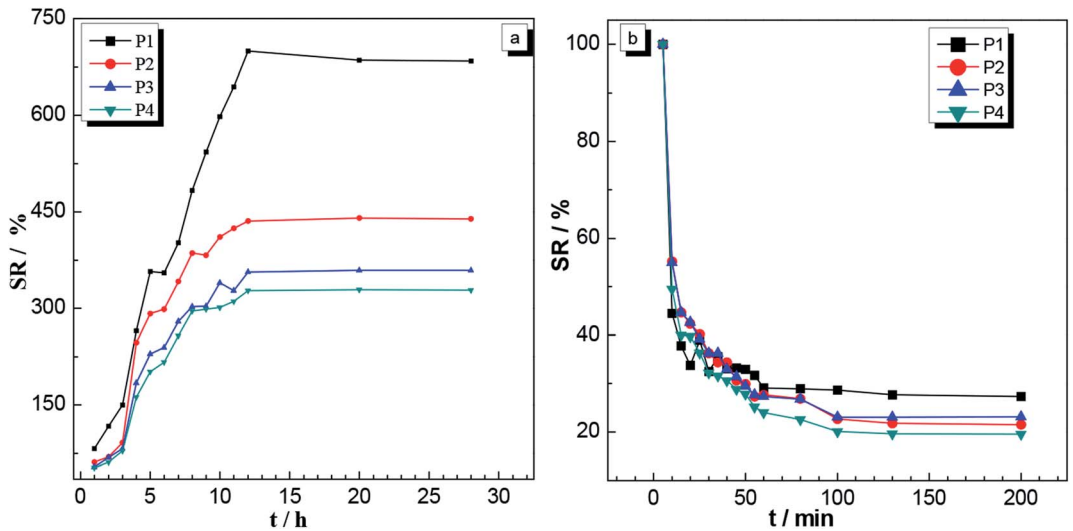

Fig. 11 (a) Swellings of the P1, P2, P3, and P4 gels in deionized water at 25 °C and pH = 7 and (b) de-swellings of the gels at 40 °C.

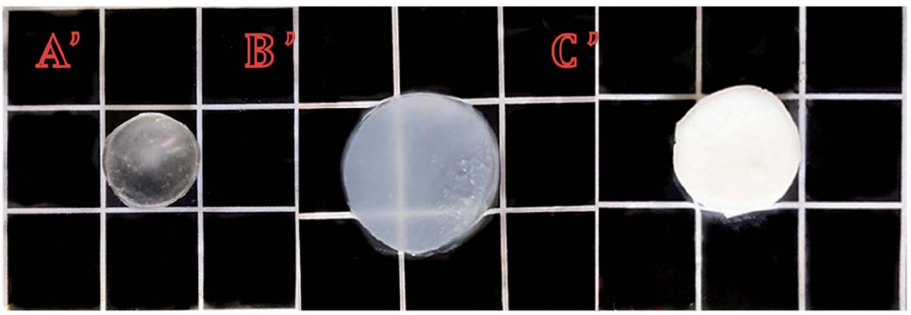

Fig. 13 Photographs taken with a digital camera of (A′) an untreated gel, (B′) gel completely swelled in a water bath at pH 7, 25 °C, and (C′) gel stabilized in a 40 °C water bath.

to study their de-swelling kinetics. As shown in Fig. 11(b), the gels tended to shrink and dehydrate at 40 °C, and the water retention was obviously reduced within 10 min. Thus, the gels were found to be temperature sensitive. When the temperature of the gels was higher than the LCST, the hydrogen bonds between the hydrophilic chains P(MEO_2MA-*co*-OEGMA) and water molecules became broken, and the P(MEO_2MA-*co*-OEGMA) chains agglomerated into a spherical shape. So the gels rapidly lost water and violently shrank, and the amount of water retained was reduced. (The experiment was repeated three times to ensure the accuracy of the data.)

3.2.6. Reversible swelling of the gels. In order to study the reversibility of the gel swelling, the P3 gel was subjected to swelling, de-swelling experiments at certain temperatures. After the gel was completely swollen, its swelling degree reached 100%. Then it was swollen, de-swollen and swollen at 25 °C and 42 °C, and a change of the curve was observed. As shown in Fig. 12, the P3 gel displayed good reversible swelling. (The experiment was repeated three times to ensure the accuracy of the data.)

Fig. 13 shows photographs of this P3 gel taken with a digital camera. (A′) shows a photograph of the untreated gel; (B′) shows a picture of the gel completely swelled in a deionized water bath at pH = 7, 25 °C; and (C′) shows a photograph after the gel was placed in a 40 °C deionized water bath. These photographs showed that after the gel was completely swollen, it shrank and whitened with increasing temperature, completely consistent with the results of 3.6.2 (a) and (b). These results illustrated the temperature sensitive nature of the gels.

3.2.7. DSEM images of cross-sections of the gels. The morphologies of the APCN gels were further studied using a desktop scanning electron microscope (DSEM). Fig. 14(A)–(D)

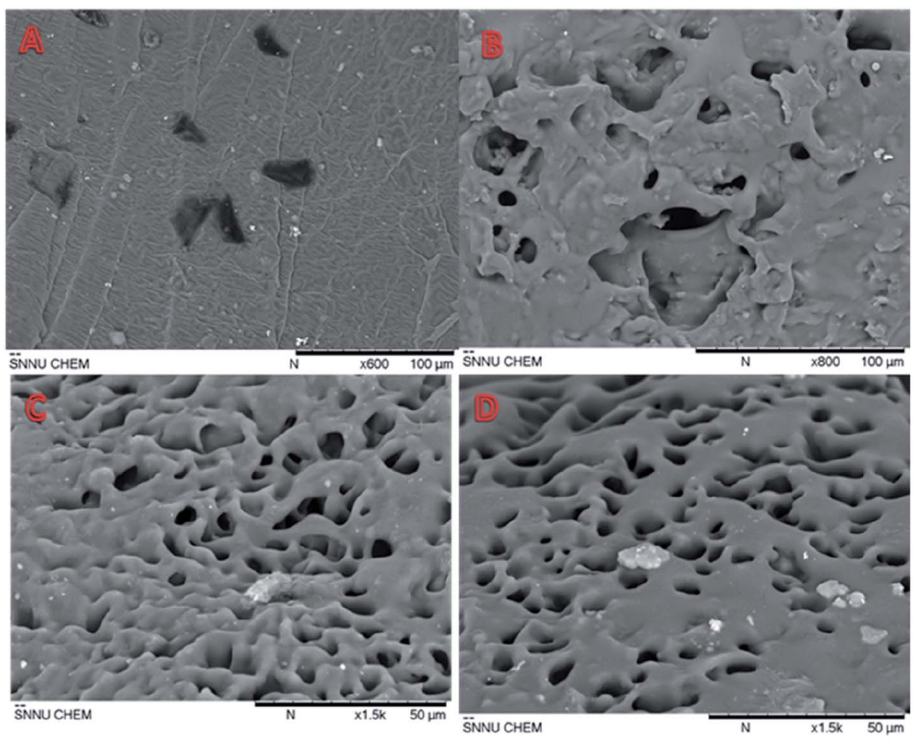

Fig. 14 DSEM images of cross-sections of completely swollen (A) P1, (B) P2, (C) P3 and (D) P4 gels at room temperature.

show images of cross-sections of the gels with different PLA stereocomplex contents. Inspection of these images showed larger pores for the gels with lower extents of PLA polymerization. This result was attributed to the gels having been formed by the physical crosslinking of PLLA and PDLA. As the amount of the stereocomplex of PLA was increased, the quantity of interaction points of hydrogen bonding between PLLA and PDLA increased, and the pore size gradually decreased, completely consistent with the conclusions drawn from the gel swelling curve in water.

4. Conclusions

APCNs were successfully synthesized by carrying out free radical copolymerization of PLLA and PDLA stereocomplex with MEO_2MA and OEGMA comonomers. A series of APCN gels with different compositions were obtained by tuning the ratio of the amount of hydrophobic macromonomer to that of the hydrophilic monomer. The appearance of characteristic XRD and DSC peaks indicated that the gel stereocomplexations were successful. The gels swelled in both the organic and aqueous phases, and the swelling behaviors of the gels were different in aqueous phases at different temperatures, indicative of the relatively high amphiphilicity and temperature sensitivity levels of the gels. DMA and thermal analysis system measurements showed that PLA was greatly improved by MEO_2MA and OEGMA, and indicated the higher mechanical strengths and better thermal performances of the amphiphilic co-network gels. These APCNs and gels may, due to their unique structures and properties, find potential biomedical applications such as in encapsulating and delivering hydrophobic drug molecules.

Conflicts of interest

There are no conflicts to declare. With the consent of all of the authors, we made corrections.

Acknowledgements

This research was supported by the National Natural Science Foundation of China (No. 21773147).

Notes and references

1 S. M. Cannizzaro and R. S. Langer, Polymeric systems for controlled drug release, *Chem. Rev.*, 1999, **99**, 3181–3198.
2 E. Chielhi and R. Solaro, Biodegradable polymeric materials, *Adv. Mater.*, 1996, **8**, 305–313.
3 H. R. Kricheldorf, M. Berl and N. Scharnagl, Poly(lacto- -nes) polymerization mechanism of metal alkoxideinitiated polymerizations of lactide and various lactones, *Macromolecules*, 1988, **21**, 286–293.
4 M. Jamshidian, E. A. Tehrany, M. Imran, M. Jacquot and S. Desobry, Poly-lacticacid: production, applications, nanocomposites, andreleasestudies, *Compr. Rev. Food Sci. Food Saf.*, 2010, **9**, 552–571.
5 P. J. Pan, L. L. Han, J. N. Bao, Q. Xie, G. R. Shan and Y. Z. Bao, Competitive stereocomplexation, homocrystallization, and polymorphic crystalline transition in poly(L-lactic acid)/poly(D-lactic acid) racemic blends: molecular weight effects, *J. Phys. Chem. B*, 2015, **119**, 6462–6470.
6 H. L. Mao, P. J. Pan, G. R. Shan and Y. Z. Bao, In situ formation and gelation mechanism of thermoresponsive stereocomplexed hydrogels upon mixing diblock and triblockpoly(lactic acid)/poly(ethylene glycol) copolymers, *J. Phys. Chem. B*, 2017, **119**, 6471–6480.
7 J. M. Zhang, H. Sato, H. Tsuji, I. Noda and Y. Ozaki, Infrared spectroscopic study of $CH_3\cdots O{=}C$ interaction during poly(L-lactide)/poly(D-lactide) stereocomplex formation, *Macromolecules*, 2005, **38**, 1822–1828.
8 Z. W. Zhao, Z. Zhang, L. Chen, Y. Cao, C. L. He and X. S. Chen, Biodegradable stereocomplex micelles based on dextran-block-polylactide as effcient drug deliveries, *Langmuir*, 2013, **29**, 13072–13080.
9 E. Gisha and C. K. S. P. Luckachan, Biodegradable polymers-areview on recent trends and emerging perspectives, *J. Polym. Environ.*, 2011, **19**, 637–676.
10 J. Slager and A. J. Domb, Biopolymer stereocomplexes, *Adv. Drug Delivery Rev.*, 2003, **55**, 549–583.
11 M. Kakuta, M. Hirata and Y. Kimura, Stereoblock polylactides as high-performance bio-based polymers, *J. Macromol. Sci., Polym. Rev.*, 2009, **49**, 107–140.
12 P. J. Pan, J. J. Yang, G. R. Shan, Y. Zh. Bao, Z. X. Weng, A. Cao, K. Yazawa and Y. Inoue, Temperature-variable FTIR and solid-state ^{13}C NMR investigations on crystalline structure and molecular dynamics of polymorphic poly(L-lactide) and poly(Llactide)/poly(D-lactide) stereocomplex, *Macromolecules*, 2012, **45**, 189–197.
13 X. S. Fan, M. Wang, D. Yuan and C. B. He, Amphiphilic conetworks and gels physically cross-linked via stereocomplexation of polylactide, *Langmuir*, 2013, **29**, 14307–14313.
14 G. Kali, S. l. Vavra, K. László and B. Iván, Thermally responsive amphiphilic conetworks and gels based on poly(*N*-isopropylacrylamide) and polyisobutylene, *Macromolecules*, 2013, **46**, 5337–5344.
15 J. F. Lutz, Thermo-switchable materials prepared using the OEGMA-platform, *Adv. Mater.*, 2011, **23**, 2237–2243.
16 J. Franc, O. Lutz and A. Hoth, Preparation of ideal PEG analogues with a tunable thermosensitivity by controlled radical copolymerization of 2-(2-methoxyethoxy)ethyl methacrylate and oligo(ethylene glycol) methacrylate, *Macromolecules*, 2006, **39**, 893–896.
17 S. T. Sun and P. Y. Wu, On the thermally reversible dynamic hydration behavior of oligo(ethylene glycol) methacrylate-based polymers in water, *Macromolecules*, 2013, **46**, 236–246.
18 J. Wu, X. Y. Shi, Z. D. Wang, F. Song, W. L. Gao and S. X. Liu, Stereocomplex Poly(Lactic Acid) Amphi- -philic Conetwork Gel with Temperature and pH Dual Sensitivity, *Polymers*, 2019, **11**, 1940.
19 M. R. Kalourkoti, E. N. Kitiri, C. S. Patrickios, E. Leontidis, M. Constantinou, G. Constantinides, X. h. Zhou and C. M. Papadakis, Double networks based on amphiphilic

cross-linked star block copolymer first conetworks and randomly cross-linked hydrophilic second networks, *Macromolecules*, 2016, **49**, 1731–1742.

20 C. Lin and I. Gitsov, Preparation and characterization of novel amphiphilic hydrogels with covalently attached drugs and fluorescent markers, *Macromolecules*, 2010, **43**, 10017–10030.

21 D. Kafouris, M. Gradzielski and C. S. Patrickios, Semisegmented amphiphilic polymer conetworks: synthesis and characterization, *Macromolecules*, 2009, **42**, 2972–2980.

22 M. D. Rikkou, E. Loizou, L. Porcar, P. Butler and C. S. Patrickios, Degradable amphiphilic end-linked conetworks with aqueous degradation rates determined by polymer topology, *Macromolecules*, 2009, **42**, 9412–9421.

23 C. A. K. Singh, B. Nutan, I. H. Raval and S. K. Jewrajka, Self-assembly of partially alkylated dextran-graft-poly [(2dimethylamino)ethyl methacrylate] copolymer facilitating hydrophobic/hydrophilic drug delivery and improving conetwork hydrogel properties, *Biomacromolecules*, 2018, **19**, 1142–1153.

24 G. Guzman, T. Nugay, I. Nugay, N. Nugay, J. Kennedy and M. Cakmak, High strength bimodal amphiphilic conetworks for immunoisolation membranes: synthesis, characterization, and properties, *Macromolecules*, 2015, **48**, 6251–6262.

25 T. Hiroi, S. Kondo, T. Sakai, E. P. Gilbert, Y. S. Han, T. H. Kim and M. Shibayama, Fabrication and structural characterization of module-assembled amphiphilic conetwork gels, *Macromolecules*, 2016, **49**, 4940–4947.

26 A. Domján, C. Fodor, S. Kovács, T. Marek, B. Iván and K. Süvegh, Anomalous swelling behavior of poly(*N*-vinylimidazole)-*l*-poly(tetrahydrofuran) amphiphilic conetwork in water studied by solid-state NMR and positron annihilation lifetime spectroscopy, *Macromolecules*, 2012, **45**, 7557–7565.

27 A. Domján, P. Mezey and J. Varga, Behavior of the interphase region of an amphiphilic polymer conetworks wollen in polar and nonpolar solvent, *Macromolecules*, 2012, **45**, 1037–1040.

28 C. Zhou, L. H. Deng, F. Yao, L. Q. Xu, J. Zhou and G. D. Fu, A well-defined amphiphilic polymer conetwork from sequence control of the cross-linking in polymer chains, *Ind. Eng. Chem. Res.*, 2014, **53**, 19239–19248.

29 S. Nakagawa, X. Li and M. Shibayama, Insight into the microscopic structure of module- assembled thermoresponsive conetwork hydrogels, *Macromolecules*, 2018, **51**, 6645–6652.

30 Ch. C. Zhou, X. Y. Zhou and X. K. Su, Noncytotoxic polycaprolactone polyethyleneglycol-ε-poly (L-lysine) triblock copolymey systhsized and self-assembled as an antibacterial drug carrier, *RSC Adv.*, 2017, **7**, 39718–39725.

31 K. J. Mochizuki and D. B. Amotz, Hydration-shell transformation of thermosensitive aqueous polymers, *J. Phys. Chem. Lett.*, 2017, **8**, 1360–1364.

32 C. Krumm, S. Konieczny, G. J. Dropalla, M. Milbradt and J. C. Tiller, Amphiphilic polymer conetworks based on end group cross-linked poly(2-oxazoline) homo- and triblock copolymers, *Macromolecules*, 2013, **46**, 3234–3245.

33 J. F. Lutz, K. Weichenhan, Ö. Akdemir and A. Hoth, About the phase transitions in aqueous solutions of thermoresponsive copolymers and hydrogels based on 2-(2-methoxyethoxy) ethyl methacrylate and oligo(ethylene glycol) methacrylate, *Macromolecules*, 2007, **40**, 2503–2508.

34 Y. Yasuyuki, K. Kawahara, K. Inamoto, S. Mitsumune, S. Ichikawa, A. Kuzuya and Y. Ohya, Biodegradable Injectable Polymer Systems Exhibiting Temperature Responsive Irreversible Sol-to-Gel Transition by Covalent Bond Formation, *ACS Biomater. Sci. Eng.*, 2017, **3**, 56–67.

35 N. M. B. Smeets, E. Bakaic, M. Patenaude and T. Hoare, Injectable and tunable poly(ethylene glycol) an alogue hydrogels based on poly(oligoethylene glycol methacrylate), *Chem. Commun.*, 2014, **50**, 3306–3309.

36 C. L. Ma, P. J. Pan, G. R. Shan, Y. Z. Bao, M. Fujita and M. Maeda, Core−shell structure, biodegradation, and drug release behavior of poly(lactic acid)/poly(ethyl- -ene glycol) block copolymer micelles tuned by macromolecular stereostructure, *Langmuir*, 2015, **31**, 1527–1536.

37 J. R. Sarasua, E. P. Robert, M. Wisniewski, A. L. Borgne and N. Spassky, Crystallization and melting behavior of polylactides, *Macromolecules*, 1998, **31**, 3895–3905.

38 J. Shao, S. Xiang, X. C. Bian, J. R. Sun, G. Li and X. S. Chen, Remarkable melting behavior of PLA stereocomplex in linear PLLA/PDLA blends, *Ind. Eng. Chem. Res.*, 2015, **54**, 2246–2253.

39 J. Bai, J. Y. Wang, W. T. Wang, H. G. Fang, Z. H. Xu, X. S. Chen and Z. G. Wang, Stereocomplexcry stallite-assisted shear-induced crystallization kinetics at a high temperature for asymmetric agglomerate biodegradable PLLA/PDLA blends, *ACS Sustainable Chem. Eng.*, 2016, **4**, 273–283.